CHAPTER 3
SPATIO-TEMPORAL VARIABILITY OF LOW-LEVEL WINTERTIME WIND OVER THE INDOCHINA PENINSULA

In this chapter, the spatial patterns and their interannual variability of wintertime low-level winds over the IDP were revealed by using the analysis of empirical orthogonal function (EOF) for complex numbers. Monthly mean wind data at 850 hPa of the Japanese 25-year reanalysis data (JRA-25) for December to February covering the period of 1979-2010 were used for the analysis. Two leading modes account for 46.6% and 13.8% of the total variance respectively. The regressed spatial patterns of wind components on the first principal component (PC1) show dominant northeasterly wind over the IDP, which are related to the EAWM circulation and connected to the cyclonic circulation near the Borneo.

To further support this notation, this section also explored the relationship between wintertime low-level wind variability over the IDP and the EAWM. Various EAWM indices defined by sea level pressure, low-level wind, and upper level wind were calculated. The correlations between the EAWM indices and the leading PC suggest the plausible linkage between wintertime low-level wind over the IDP and EAWM predominantly via the wind circulation. This study also performed correlation analysis on relationship between the leading mode of winter monsoon representing the northeast (NE) monsoon over the IDP and sea surface temperature anomaly (SSTA).

The results show that there is more significant relationship between PC1 and SSTA in the Pacific Ocean than that of the Indian Ocean. In addition, there is an association between PC1 and Niño 3.4 index from at least three previous months to three following months, and not found with the dipole mode index. This indicates that there is a linkage between the NE monsoon over the IDP and EAWM, and a relationship with SSTA in the Pacific Ocean. These results provide useful information to possibly indicate the NE monsoon variability over the IDP using Niño 3.4 index, and fulfill understanding on winter monsoon variability over the IDP.

3.1 Data and Analytical Methods

The monthly gridded 850 hPa wind of the JRA-25 data set with 1.25°×1.25° horizontal resolution (Onogi, 2007) during the boreal winter months (December-January-

February) covering the period of 1979-2010 were used for this study. The wind at 850 hPa data were extracted for the IDP region (5°-30°N, 90°-110°E) to analyse the dominant spatio-temporal modes by the EOF method.

3.1.1 The JRA-25 Data and Its Quality Control

The JRA-25 data set is a long-term global atmospheric reanalysis using the Japan Meteorological Agency numerical assimilation system. The data begins in 1979 to present. The data has 1.25°×1.25° horizontal resolution, 40 vertical layers with a top layer at 0.4 hPa level, and 6-hourly of the finest temporal resolution. The data set is the first reanalysis data establishing and focusing in Eastern Asia and Tropics to support climate research, operational monitoring, and forecasts. There are many observation data sets used for the assimilation that are conventional data, and satellite and remote-sensing data as shown in Figure 3.1. The conventional data is the data were directly observed in land, marine observation, aviation observation, and upper air observation that including the data of wind profile retrievals surrounding tropical cyclone and Chinese snow data.

The satellite and remote-sensing data are the data of the Television and InfraRed Observation Satellite (TIROS) Operational Vertical Sounder (TOVS), the Advanced TOVS (ATOVS), the data of Special Sensor of Microwave Imager (SSMI) precipitable water, the Atmospheric Motion Vector (AMV) data from Geostationary Meteorological Satellites, GMS-3 to GMS-5, of the Japan Meteorological Agency (JMA), and data from other satellites that are the European Remote-sensing Satellites (ERS), NASA’s Quick Scatterometer (QuikSCAT), and the Moderate Resolution Imaging Spectroradiometer (MODIS) (Onogi, 2007).

For quality control (QC), there are many QC processes that are similar to operational techniques by the JMA, as shown in Table 3.1. The basic method, which is climatologically checks are used for most of data types. Track check is performed to check quality of data from the moving stations that are ships, drifting buoys, and airship. The duplication of observation data were considered, and they were prioritized for selection. Some of data are extremely and problematic. Such data are blacklisted, and to be excluded for used in advance processes. For the radiosonde temperature, the bias correction were used, based on the historical performance of radiosondes that perhaps differences between countries or regions. The bias correction was also considered as the mean departure of the observation from the optimal solution of one-dimensional variational method, and used as a correction (Onogi, 2007).

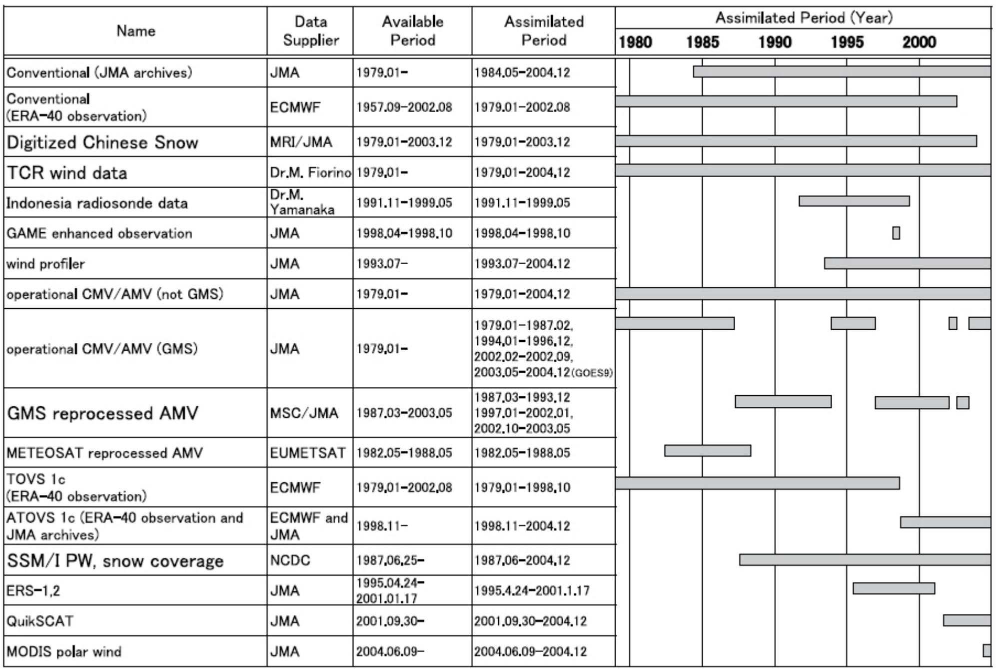

Name	Data Supplier	Available Period	Assimilated Period	Assimilated Period (Year) 1980 1985 1990 1995 2000
Conventional (JMA archives)	JMA	1979.01–	1984.05–2004.12	
Conventional (ERA–40 observation)	ECMWF	1957.09–2002.08	1979.01–2002.08	
Digitized Chinese Snow	MRI/JMA	1979.01–2003.12	1979.01–2003.12	
TCR wind data	Dr.M. Fiorino	1979.01–	1979.01–2004.12	
Indonesia radiosonde data	Dr.M. Yamanaka	1991.11–1999.05	1991.11–1999.05	
GAME enhanced observation	JMA	1998.04–1998.10	1998.04–1998.10	
wind profiler	JMA	1993.07–	1993.07–2004.12	
operational CMV/AMV (not GMS)	JMA	1979.01–	1979.01–2004.12	
operational CMV/AMV (GMS)	JMA	1979.01–	1979.01–1987.02, 1994.01–1996.12, 2002.02–2002.09, 2003.05–2004.12(GOES9)	
GMS reprocessed AMV	MSC/JMA	1987.03–2003.05	1987.03–1993.12 1997.01–2002.01, 2002.10–2003.05	
METEOSAT reprocessed AMV	EUMETSAT	1982.05–1988.05	1982.05–1988.05	
TOVS 1c (ERA–40 observation)	ECMWF	1979.01–2002.08	1979.01–1998.10	
ATOVS 1c (ERA–40 observation and JMA archives)	ECMWF and JMA	1998.11–	1998.11–2004.12	
SSM/I PW, snow coverage	NCDC	1987.06.25–	1987.06–2004.12	
ERS–1,2	JMA	1995.04.24–2001.01.17	1995.4.24–2001.1.17	
QuikSCAT	JMA	2001.09.30–	2001.09.30–2004.12	
MODIS polar wind	JMA	2004.06.09–	2004.06.09–2004.12	

Figure 3.1: Data used in assimilation for the JRA-25 reanalysis (Onogi, 2007).

Table 3.1: Quality control procedures used for JRA-25 data establishment (Onogi, 2007).

Major QC processes	Target data type
Blacklist	Conventional and satellite wind
TOVS/ATOVS blacklist	TOVS/ATOVS
Climatological check	All data
Track check	SHIP, drifting buoy, aviation
Consistency between parameters	SYNOP, SHIP
Wind speed correction depends on elevation of instrument	SHIP
Radiosonde bias correction	Radiosonde
Vertical consistency of temperature	Radiosonde
Vertical consistency of wind	Radiosonde
TOVS/ATOVS bias correction	TOVS/ATOVS
TOVS/ATOVS 1D-Var	TOVS/ATOVS
Gross error check (dynamic QC)	Conventional and satellite wind
Space consistency check (dynamic QC)	Conventional and satellite wind
Group QC	Sea surface wind
SSM/I quality check	SSM/I
Reassignment of vertical levels	Satellite wind data of a part of satellites

3.1.2 Analytical Methods

Some previous studies used EOF to analyze wind components by forming in complex numbers (Hardy, 1977; Legler, 1983; Zhao, 2010). The wind vector in complex exponential form is defined by the direction measuring from East to North, and the magnitude of vector as the wind speed (Hardy, 1978). Thus, the wind vector in complex rectangular form consists of the zonal and meridional wind components represented by the real and imaginary parts, respectively. In this study, the wind components at 850 hPa were used to form a complex numbers in a rectangular form respected to the zonal and meridional axes. A matrix $\mathbf{S}$ of dimension $N\times M$ is a sample matrix, where the elements of $\mathbf{S}$ defined as

$$e_{km} = u'_{km} + iv'_{km}\,, \tag{3.1}$$

where $u',\ v',\ k = 1,\ ...N,$ and $m = 1,\ ...M,$ denote for zonal wind anomaly, meridional wind anomaly, the location and time, respectively. To analyse a matrix of complex number elements by EOF, a symmetric composition of complex numbers except for diagonal elements that named the Hermitian matrix ($\mathbf{H}$) is required. There are important properties of $\mathbf{H}$, which are as follows: (1) Eigenvalues are real, (2) eigenvectors corresponding to the distinct eigenvalues meet orthogonality, and (3) it is unitarily diagonalizable. The matrix S is used to form a Hermitian matrix for the analysis as:

The method has been often used for analyses of scalar variables such as precipitation, sea surface temperature, and temperature (Diaz, 2001; Limsakul, 2008; Li, 2010; Limsakul, 2010). The important procedure for the analysis is data forming for gridded data, which described by Hannachi (2007) as follows:

$$\mathbf{H} = M^{-1}\mathbf{S}\mathbf{S}^{\dagger}\,, \tag{3.2}$$

where $\mathbf{H}$ is the Hermitian matrix, and is the complex conjugate transpose of the matrix.

Therefore, eigenvectors ($\hat{\mathbf{E}}_j$) are determined by:

$$\mathbf{H}\mathbf{E}_j = \lambda_j \hat{\mathbf{E}}_j\,, \quad j = 1,\ ...,N\,, \tag{3.3}$$

and satisfy the unitary condition:

$$\hat{\mathbf{E}}_i^{\dagger}\hat{\mathbf{E}}_j = \delta_{ij}, \quad i, j = 1, ..., N, \tag{3.3}$$

where $\hat{\mathbf{E}}_i^{\dagger}$ is the complex conjugate transpose of $\hat{\mathbf{E}}_i$, and δ_{ij} is the Kronecker delta function. The eigenvalues λ_j are real, and the complete set of N eigenvectors meet orthogonality condition due to property of $\mathbf{H}$. The eigenvectors $\hat{\mathbf{E}}_j$ are called modes of empirical orthogonal analysis. They are used to expand data as:

$$\mathbf{S}_m = \sum_{k=1}^{N} c_{km}\hat{\mathbf{E}}_k, \quad m = 1, ..., M, \tag{3.5}$$

where

$$c_{km} = \hat{\mathbf{E}}_k.\mathbf{S}_m, \quad k = 1, ..., N; m = 1, ..., M, \tag{3.5}$$

The c_{km} is unique and in complex number form (hereafter referred to as the principal component: PC), Nevertheless, there is an arbitrary phase factor (θ_k) associated to the k^{th} eigenvector, the set of vectors is $\exp(i\theta_k)\hat{\mathbf{E}}_k$. It was considered by taking this into account by choosing θ_k when the mean value of the argument of c_{km} nearly to zero to orient corresponding eigenvector and PC (Hardy, 1978). Thus, the real component variation represents varying magnitudes of corresponding eigenvector elements, whereas the imaginary part perpendicular to the vector indicates the strength of the vector rotation in a counter-clockwise direction (Legler, 1983).

Since the EAWM is the prominent climate feature during the winter season, it is important to reveal the relationship between the winter monsoon over the IDP and the EAWM. The leading PCs of the wintertime low-level winds over the IDP given by EOF analysis of complex numbers were then used to represent the variability of the winter monsoon over the IDP in terms of magnitude and rotation. Any relationships of them were explored based on correlation analysis between the two leading PCs and the EAWM indices derived from wind fields and SLP. Eight EAWM indices were calculated base on the JRA-25 data for the boreal winter period. method.

3.1.3 EAWM indices

There are many indices describing the EAWM behaviour, but the indices derived from the East Asian trough related to the climate mode in the middle latitudes that is AO. Also indices derived from the wind fields and SLP, are quite more related to the tropical climate feature than that (Wang, 2010). Eight EAWM indices were calculated base on the JRA-25 data for the boreal winter period as shown in Figure 3.2 with the IDP domain. An EAWM intensity index (EAWMI) introduced by (Chen, 2000) is determined by averaging the meridional wind component at 10 m over the region of the East China Sea (25°-40°N, 120°-140°E) and the South China Sea (10°-25°N, 110°-130°E). The second and the third indices are the low-latitudinal EAWM (EAWM-L) and the mid-high latitudinal EAWM (EAWM-M) indices representing meridional wind averages over the low-latitude area (10°-25°N, 105°-135°E) and the mid-high latitude area (30°-50°, 110°-125°E), respectively (Liu, 2012). The forth index is the v-index (VI) introduced by Ji (1997) represents a mean value of meridional wind component at 1000 hPa level over the area of 10°-30°N, 115°-130°E. The fifth index is a unified index (UMI) introduced by Lu (1999), representing an average of meridional wind component at 1000 hPa level over the South China Sea (7.5°-20°N, 107.5°-120°E). The sixth is the EAWM index defined by the sum of the zonal SLP differences (110°E minus 160°E) from 20°N to 50°N, known as the monsoon index (MI), hereafter referred to as MI1 (Xu, 2001). The seventh index is similar to MI1, but considers from 20°N to 70°N, and hereafter referred to as MI2 (Wu, 2002). The last index, which is U300 introduced by Jhun (2004), defined as the difference in the area-averaged zonal wind speed at the 300-hPa level between a region (27.58°-37.58°N, 110°-170°E) and a region (50°-60°N, 80°-140°E).

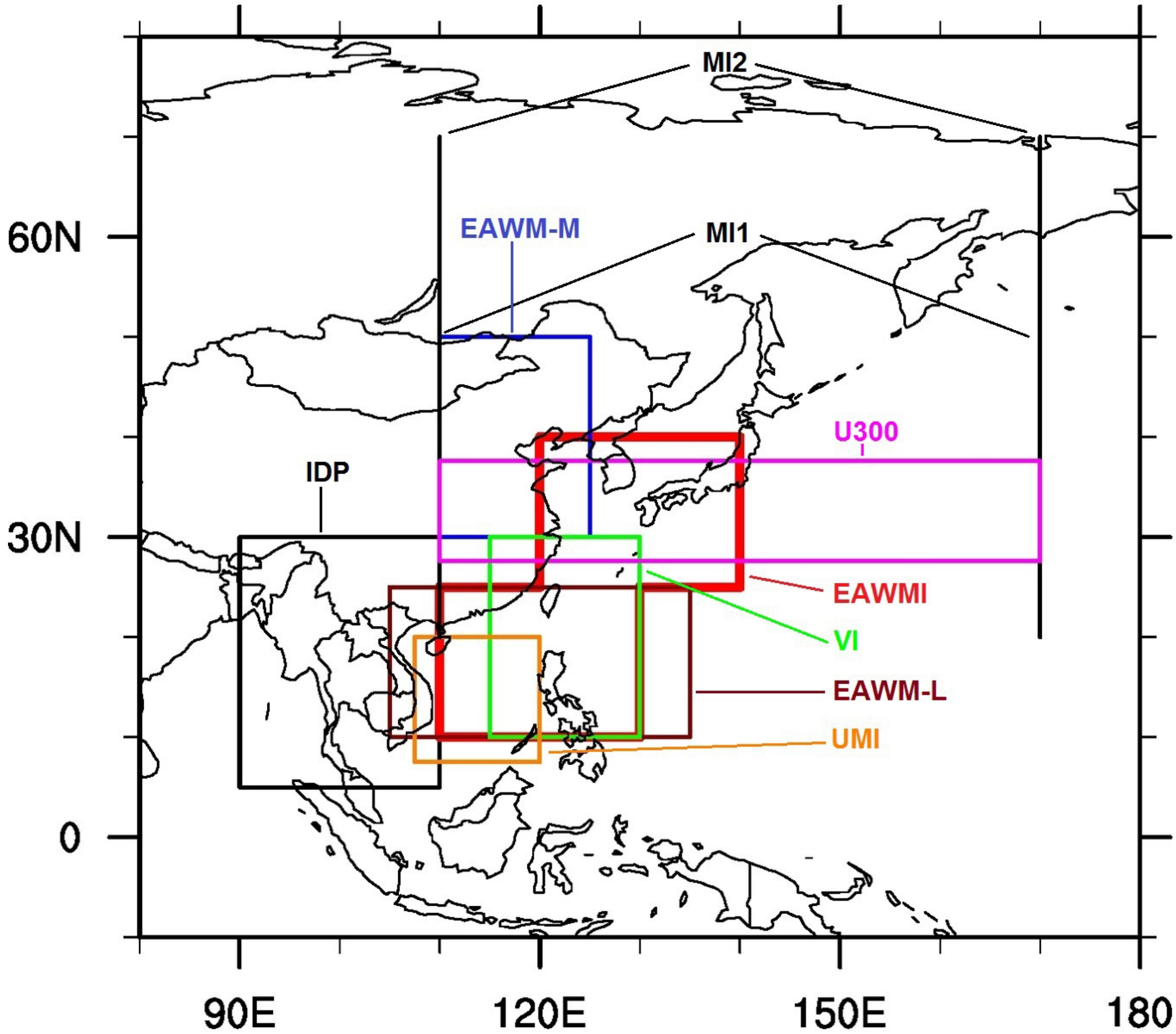

Figure 3.2: The study area of the Indochina Peninsula (IDP), and areas used for index calculations. Red, brown, blue, green, orange, and purple bounded areas represent EAWMI, EAWM-L, EAWM-M, VI, UMI, and U300 indices, respectively, whereas black lines from 20°N to 70°N and 20°N to 50°N show MI1 and MI2 index constructions.

3.2 Variability of Wintertime Low-Level Wind over the IDP

The eigenvector and PC given by the analysis are in complex exponential form used to present spatial patterns and variations in magnitude and angle of a wind vector (Hardy, 1978; Legler, 1983). All the elements of the k^{th} EOF mode are used to present the corresponding spatial pattern, whereas the corresponding PC presents the corresponding time series. In creasing of the primary component (a real part) of PC indicates lengthening of vectors or affecting the magnitude of vectors given by the corresponding eigenvector, whereas increasing of the secondary component (an imaginary part) means the varying of orientation in counter-clockwise direction of all vectors given by the corresponding eigenvector (Legler, 1983). Here after the primary and secondary PCs denote as PCpri and PCsec, respectively.

The dominant modes of wintertime low-level wind anomalies over the IDP are given by the analysis. These are the first and second modes account for 46.6% and 13.8% of the total variance, respectively (Figure 3.3). The corresponding PC time series that consist of primary and secondary components show in Figure 3.4, and the values present in an Appendix A.

(a) Mode1 (b) Mode2

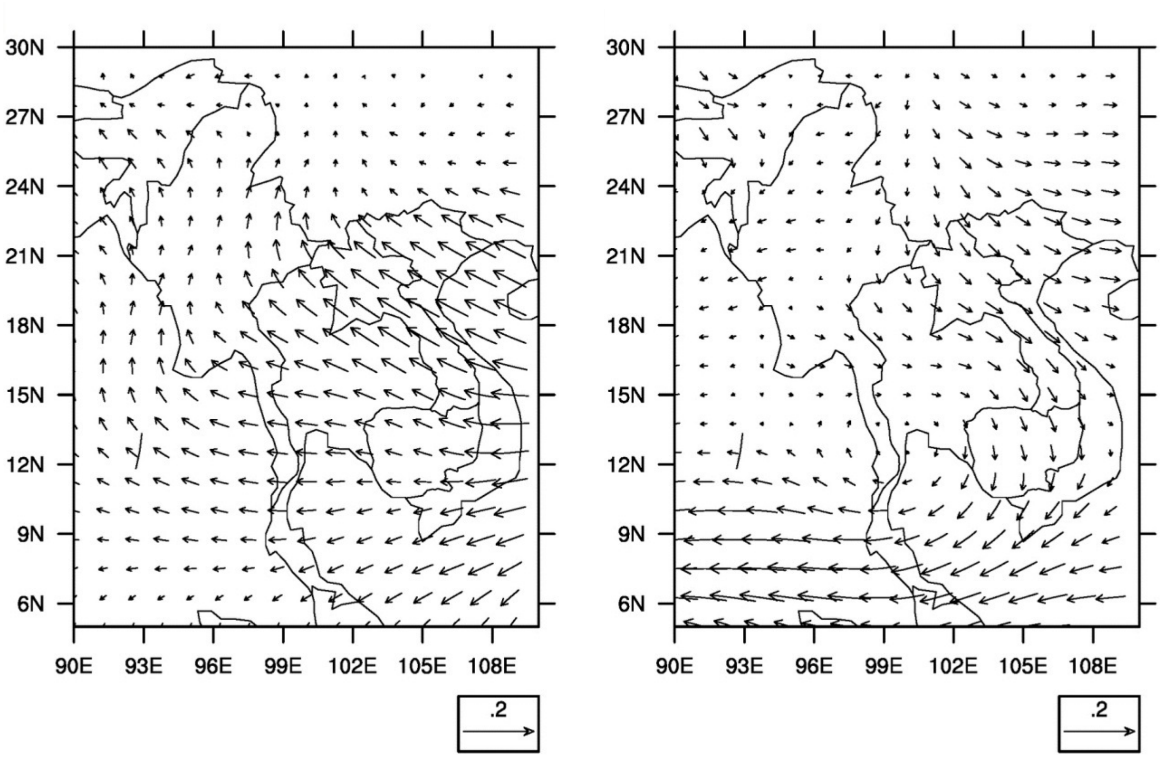

Figure 3.3: The spatial patterns of (a) the first eigenvector and (b) the second eigenvector. The vector size is relative to wind speed.

For the leading mode (Mode1), the spatial pattern shows the wind blowing from the East to the West, and the wind splits into two branches that turn northward and southward over the upper and lower 10°N areas, respectively. Nevertheless, the spatial pattern does not give enough information to describe its variability. The time series of the PC1pri and PC1sec of the first principal component exhibit large interannual variation in magnitude and rotation of the leading mode, and it correlates significantly to each other (Figure 3.4a).

The correlation coefficient between PC1pri and PC1sec is 0.75 with the 0.01 significant level that indicates the variation in magnitude and rotation significant correlated to each other, and the phase between magnitude and rotation components does not change in time. Therefore, oscillations of PC1s are possibly affected by the same factor. They should present the similar important wind patterns when performing regression of wind components on both PC1s. The spatial pattern was constructed by regressions of zonal and meridional wind anomalies on PC1pri to present the wind pattern affecting the magnitude of Mode1, whereas the regression of the zonal and meridional wind components on PC1sec present the wind pattern affecting the Mode1 orientation. Both of regressed wind patterns show northeasterly wind (Figures 3.5a and 3.5b) that means the increasing in positive direction of both PC1s related to enhancing of northeasterly wind over the IDP. This result indicates the variability of EOF1 in terms of magnitude and rotation related to the strength of northeasterly wind. Thus, it can say that the first mode of wind variability over the IDP influenced from the northeasterly wind.

(a) PC1

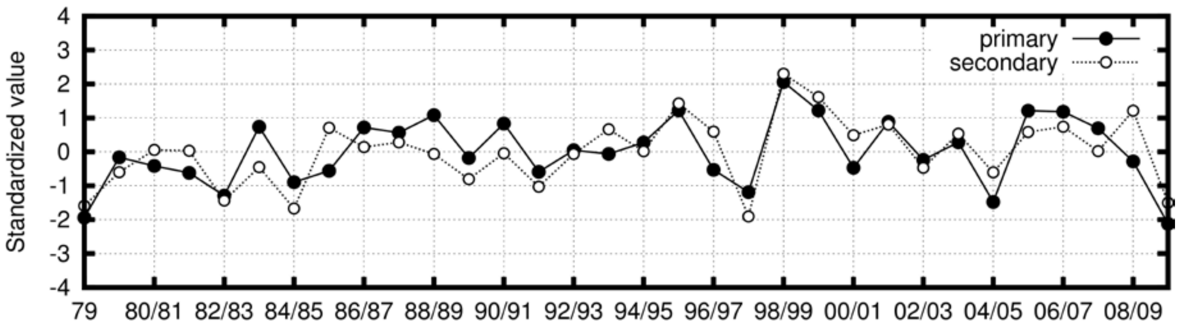

(b) PC2

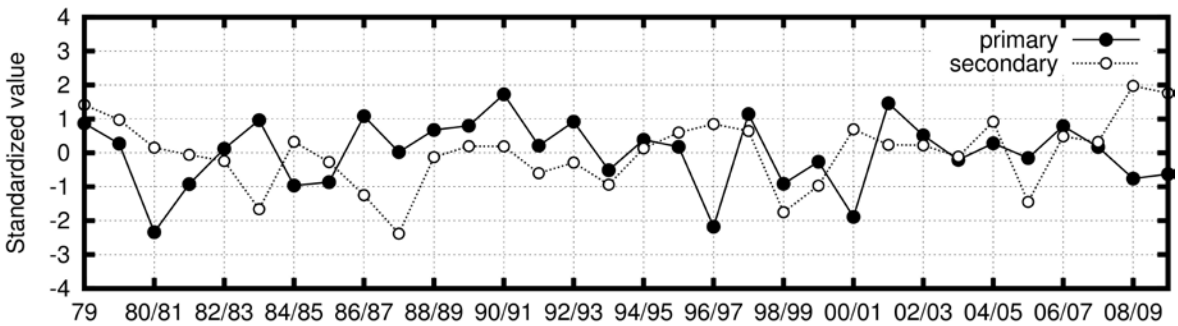

Figure 3.4: Temporal variations of primary component (solid line with black circle) and secondary component (dash line with white circle) of (a) PC1 and (b) PC2.

(a) Regression of wind on PC1pri

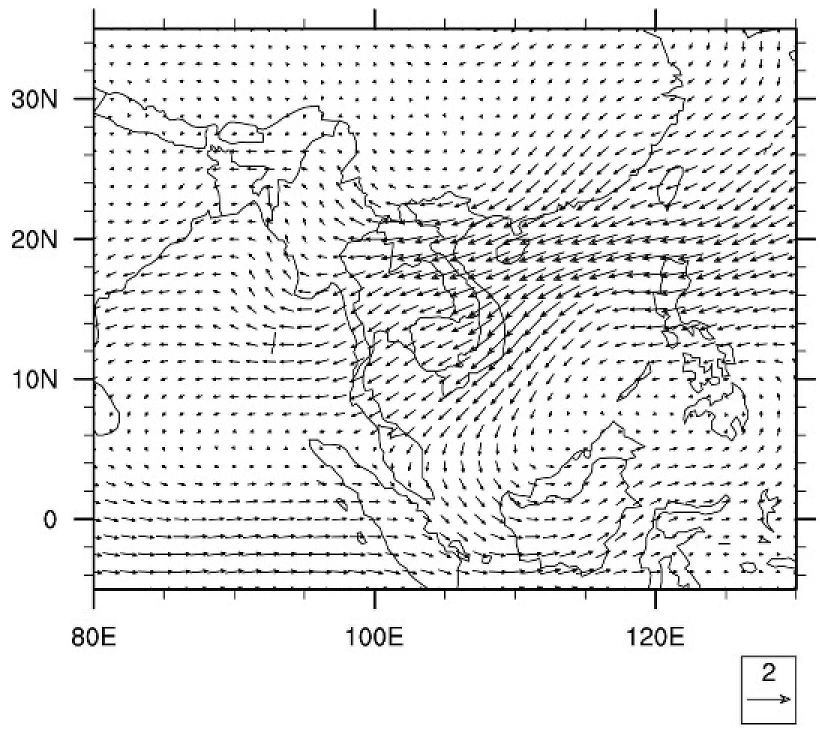

(b) Regression of wind on PC1sec

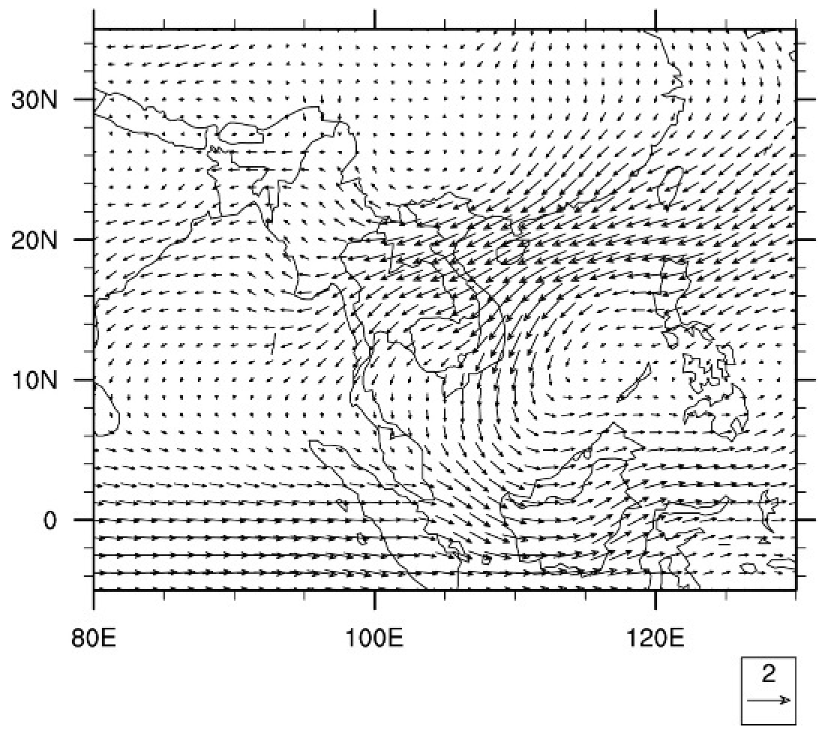

Figure 3.5: Regression maps of winter (DJF) 850-hPa wind components on (a) the primary part and (b) the secondary part of the first leading principal component (unit is m/s).

The correlations were examined for maps of correlations between PC1s (PC1pri and PC1sec) and low-level winds (zonal and meridional components) in order to investigate significant areas to ensure the relation between the northeasterly wind and the variability in magnitude (PC1pri) and rotation (PC1sec). The maps show significant negative correlations between PC1s and the zonal wind over the South China Sea (SCS) and most parts of IDP, excepting the southern tip of IDP (Figures 3.6a and 3.6b). For meridional wind, the negative correlation between the meridional wind and PC1s indicates that the northerly wind prevails over most areas of the IDP, the coastline of China, and the SCS (Figures 3.6c and 3.6d), when PC1s are positive. Our results suggest that variations in magnitude and rotation of EOF1 representing by the both PC1s related significantly to the change of northeasterly wind over the IDP and the SCS.

One of the principal EAWM characteristics shows northeasterly winds blowing along the coast of China, penetrating to the SCS, and affecting tropical areas (Chen, 2000). During strong EAWM phase, the Hadley cell in western Pacific (WPHC) shows strengthening in air ascending at the Equator, approximately, and turns poleward in the upper level, then descends in the west North Pacific, after that blows from the mid latitude to the Tropic in the low level (Zeng, 2011). Thus, the ascending induces more air travelling from midlatitude to low latitude. This indicates the northeasterly wind over the coast of China becomes stronger during strong phase of the EAWM that exerts more influence affecting the wind variability of the leading mode over the IDP. In addition, the strengthening northeasterly wind shows a connection and interannual influence to the cyclonic circulation near the Borneo (Figure 3.5).

These results agree with the studies of Juneng (2007) and Chang (2005), indicating that northeasterly wind over the northwest quadrant of the vortex may interact with a synoptic scale feature, known as the Borneo vortex located over the northern Borneo. It is found that the cyclonic vortex plays a crucial role in enhancing rainfall over eastern Malaysia Peninsular due to low-level moisture convergence (Juneng, 2007; Chang, 2005). Therefore, there is a suspicion that does the northeasterly wind affecting leading mode of wind over the IDP related to the EAWM whether or not? Because the increasing of PC1s correlated to enhancement of northeasterly wind, and the negative EAWM index derived by low-level wind means strong phase of EAWM that strengthening of northeasterly wind over the coast of China, the PC1s should presents some correlations with the EAWM index in negative direction.

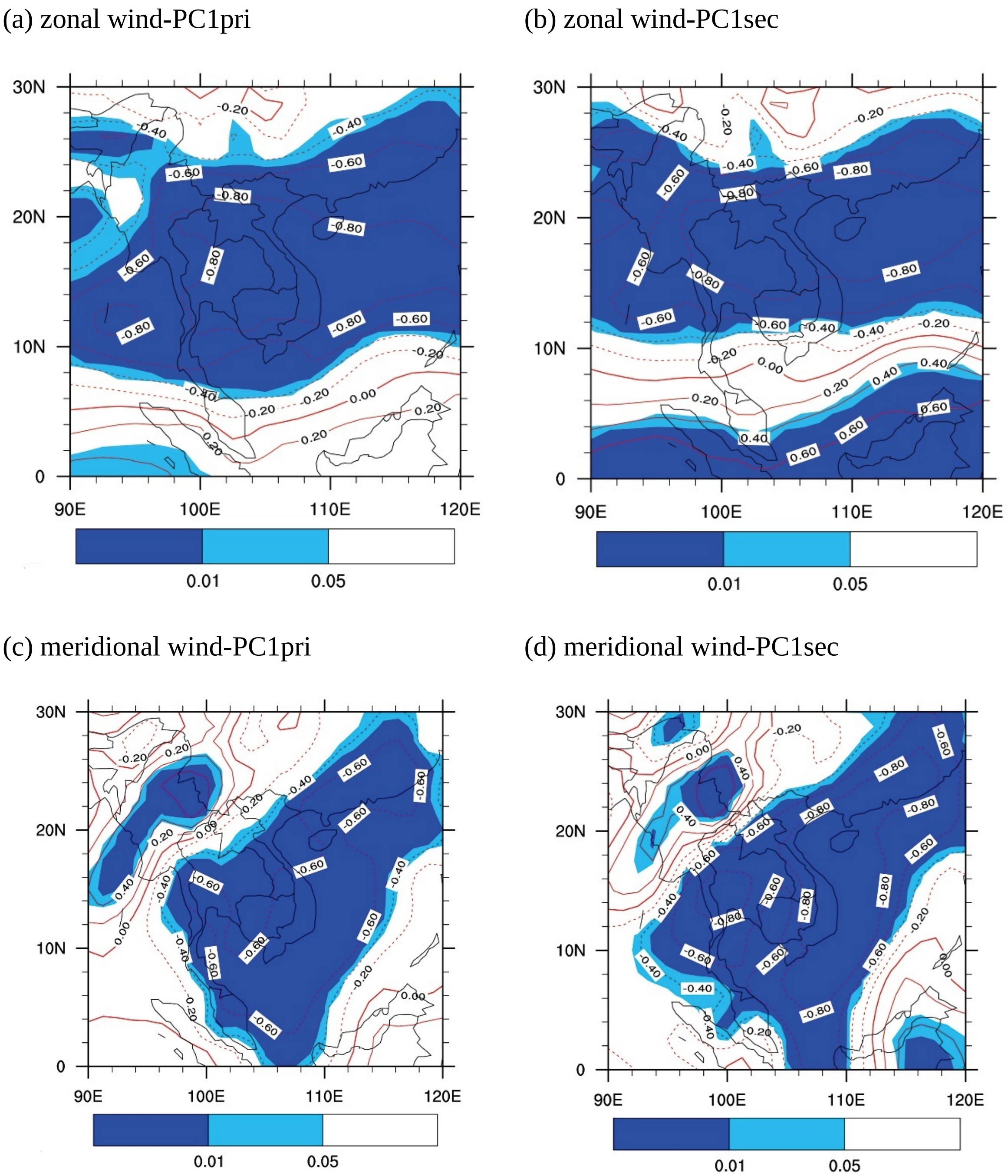

Figure 3.6: Correlation coefficients between (a) zonal wind and the primary part of the first leading principal component, (b) same as (a) but for the secondary part, (c) and (d) are similar to (a) and (b), respectively except for meridional wind. Contour line represents correlation coefficient, and the dark and light blue areas denote the significant correlations at levels 0.01 and 0.05, respectively.

The second mode (Mode2) exhibited winds blowing southward over the northern IDP, and strong easterly winds over the southern IDP (Figure 3.7a). The corresponding PC2s in terms of magnitude and orientation did not show a significant correlation (r = 0:10; p > 0:05) to each other (Figure 3.7b) that indicates the phase between them change in time, and the magnitude component of Mode2 does not significant correlated with the rotation component. The correlation pattern of PC2pri representing magnitude component on zonal wind shows strong correlation over the southern IDP, whereas the correlation between PC2sec representing the orientation component does not show significant correlation over the southern IDP, but shows weaker correlation over some areas of the northern IDP (Figures 3.8a and 3.8b). Whereas the meridional wind component does not show large significant correlation with PC2s, comparing to the zonal wind (Figures 3.8c and 3.8d). Thus, the rotation will not much affect on the strong easterly wind presented by Mode2. These indicate that the regression pattern of zonal and meridional wind components on the PC2pri should present a mode of strong zonal wind over the southern IDP, whereas the regression of wind components on the PC2sec should not present prevailing wind patterns due to the non-significant weak influence of the rotation. Figures 3.8a and 3.8b show strong easterly wind over the southern IDP and none of prevailing wind pattern corresponding to PC2pri and PC2sec, respectively. The significant mode presents strong easterly wind over the southern IDP, which should not related to the major climate feature during boreal winter, EAWM, and should not shows evidence in further analysis on examination of the relationship with the EAWM.

In summary, wintertime low-level winds over the IDP show two leading modes as evidenced by the EOF analysis of complex numbers. The Mode1 represents the mode affecting by the northeasterly wind that is the major characteristic of the EAWM. The strengthened northeasterly wind shows a connection to the cyclonic circulation that is, to some extent, related to EAWM. The second one is the easterly wind mode. This mode appears to have a non significant role in relationship with the EAWM over the IDP. There are some questions to give more understanding of wintertime wind variability over the IDP. Does the first mode have a connection with the EAWM, and whether the second mode related to the EAWM or not? If so, it should not show some evidence with the EAWM.

(a) Regression of wind on PC2pri

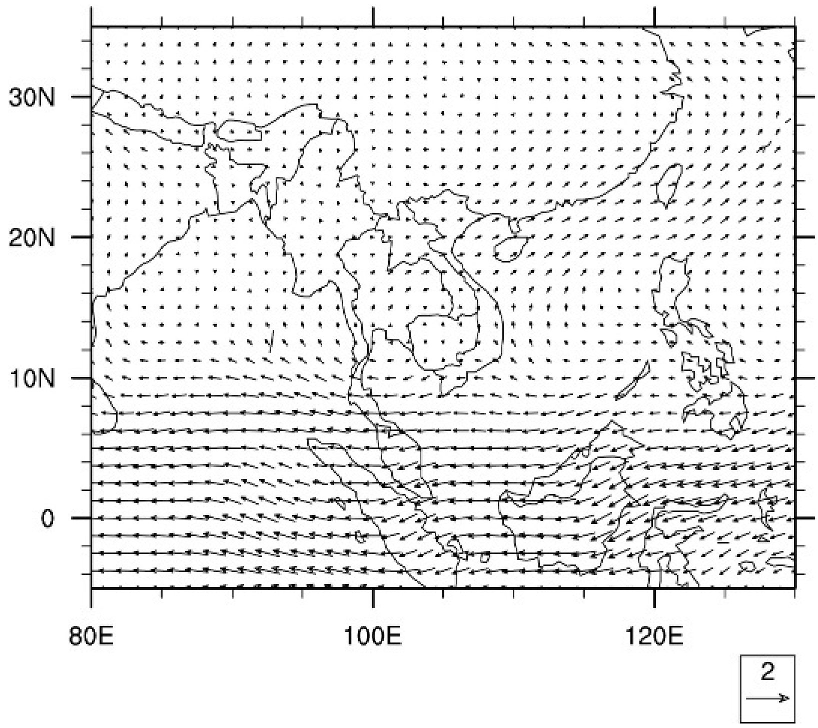

(b) Regression of wind on PC2sec

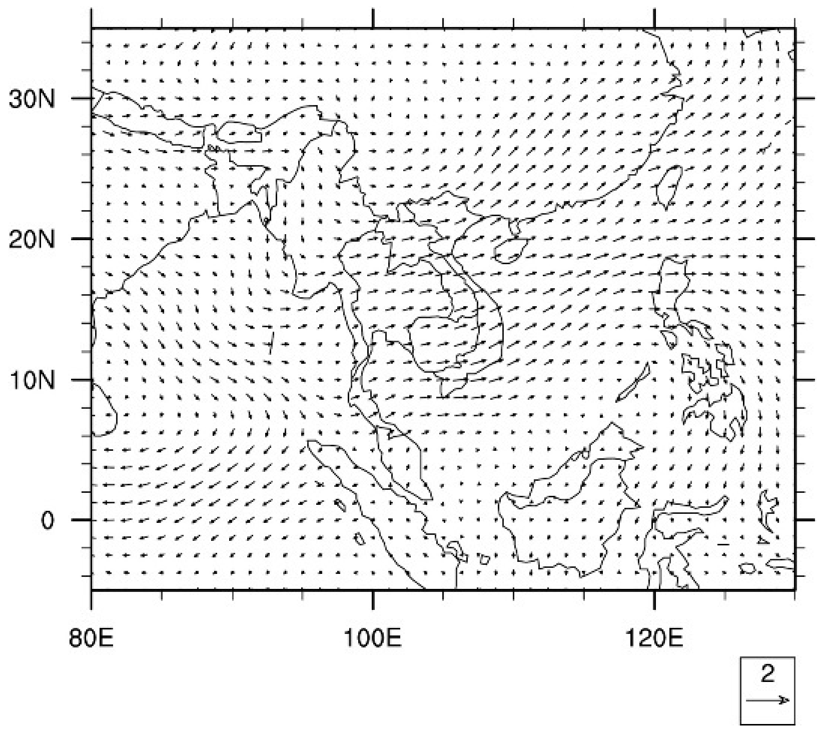

Figure 3.7: Regression maps of winter (DJF) 850-hPa wind components on (a) the primary part and (b) the secondary part of the second leading principal components (unit is m/s).

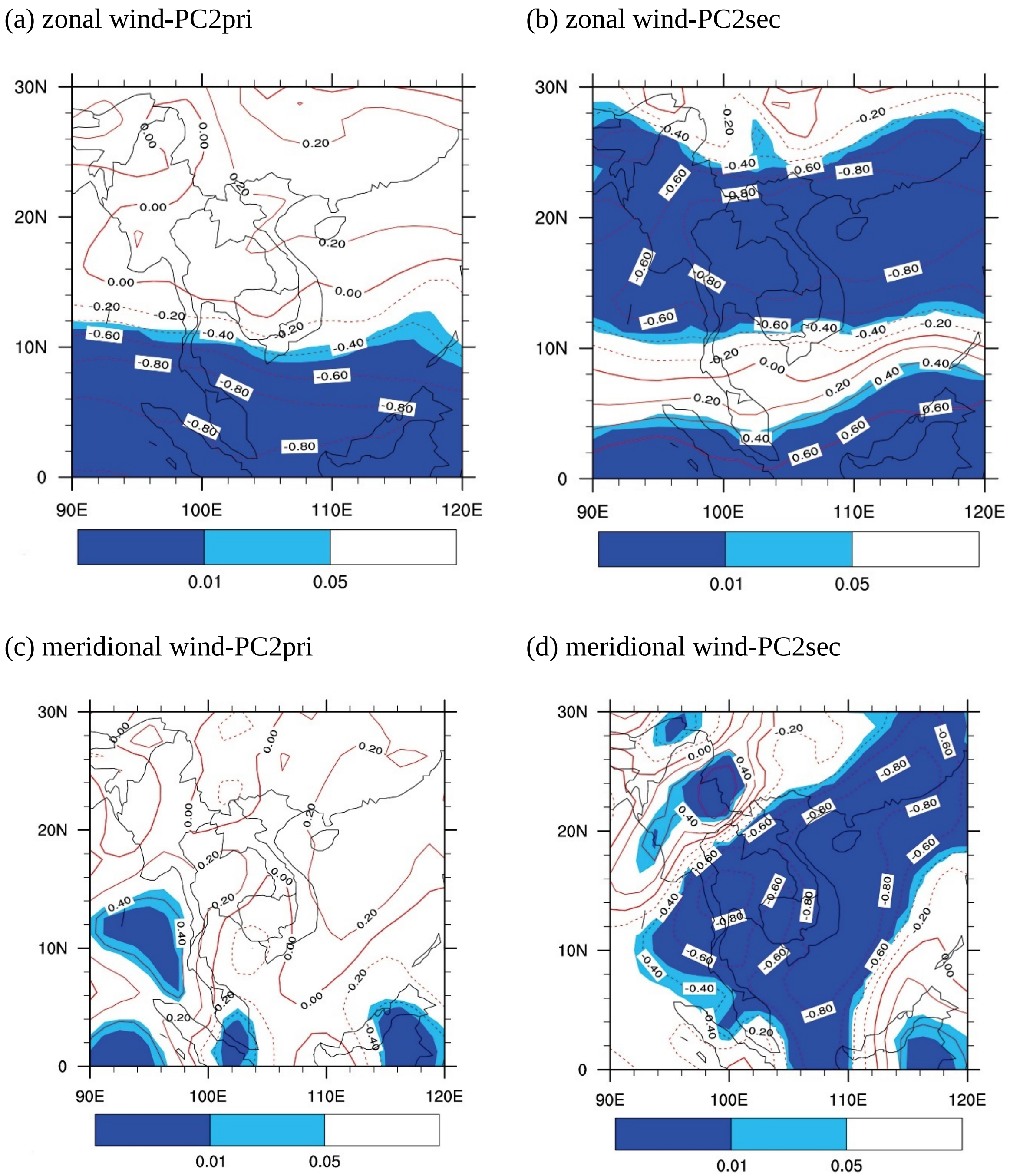

Figure 3.8: Correlation maps between (a) zonal wind and the real part of the second leading principal component, (b) same as (a) but for the imaginary part, (c) and (d) are similar to (a) and (b), respectively except for meridional wind. Contour line represents correlation coefficient, and the dark and light blue areas denote the significant correlations at levels 0.01 and 0.05, respectively.

3.3 The Relation with EAWM Indices

Basically, EAWM has been quantitatively characterized by changes in wind circulation and the SLP gradient. To measure its intensity and variability of the EAWM, therefore, the indices derived based on many aspects of these atmospheric variables were introduced. The indices can be divided into four different categories (Wang, 2010). Firstly, the EAWM intensity is represented by low-level wind that flows along the East Asia coasts. It does not influence only East Asia, but it also affects the tropical region. The indices of this category are the best among other categories that shows a good correlation with ENSO (Wang, 2010). The second category is the indices derived from the pressure gradient resulted from the difference between SH and Aleutian low (AL) influences (Wang, 2010). The relation between the fist and second category indices are highly correlated, particular the correlation between indices derived from wind at 10m and SLP (Hui, 2007). The third category is the indices related to upper level wind over East Asia, which capturing the upper tropospheric East Asian jet stream. The last group of indices related to the East Asian trough shows high correlation with the index derived from the upper level wind (Hui, 2007), and well correlation to Arctic Oscillation (AO) (Wang, 2010) that influences on the trough at 500 hPa rather than that of SH (Wu, 2002).

Since the IDP is located in the tropics and far from the Arctic region, the indices derived from low-level winds, SLP, and upper-level winds were selected. Those indices are the low-level wind indices introduced by Ji (1997), Lu (1999), Chen (2000), and Liu (2012) named as VI, UMI, EAWMI, and EAWM-L and EAWM-M, respectively, next is the indices derived from SLP introduced by Xu (2001) and Wu (2002) named MI1 and MI2, respectively, finally the index derived from upper level wind by Jhun (2004) named as U300, were used to investigate the connection between wintertime low-level wind over IDP and EAWM.

The indices were calculated for the study period following the original procedures using the JRA-25 data set. The time series of EAWM indices are shown in Appendix B. The correlation coefficients between PCs and the EAWM indices are shown in Table 3.2. They were considered with the influence of the first order auto correlation. Note that the indices derived from meridional wind are presented in the opposite sign of the original indices because the negative values denote the meridional wind blowing southward, which is consistent with the spatial patterns of wintertime low-level wind over the IDP. The correlations of PC1s to the EAWM indices are mostly statistical significant at 95%

confident level, compared to those of PC2. Thus, the significant level of correlation coefficients between PC1s and EAWM indices were recalculated with consideration of effective sample sizes. The given results do not affect the previous results, and related data shown in an Appendix C.

Further examination reveals that the indices derived from meridional winds mostly show stronger association than do others. It is suggested that the northeasterly wind (as shown in Figures. 3.5a and 3.5b) influencing wintertime wind variability of the IDP has a connection with EAWM. The index concerning on the mid-high latitude (EAWM-M) has less correlation with PC1s than the indices concerning low latitude (EAWMI, EAWM-L, UMI, and VI). It agrees with the different features of EAWM between mid-high and low latitudes, because anomalous northeasterly wind is significantly reflected by the index derived from low latitude wind (EAWM-L) than the index derived mid-high latitude wind (Liu, 2012). For the upper-wind, it has shown some correlations with the U300 index. However, the correlation coefficient is not strong, compared to low-level wind at low latitude, and it is quite closed to the correlation coefficient for the EAWM-M index. The reason of this nearness is that the U300 was defined for mid-latitude East Asia (Jhun, 2004).

A possible cause of higher correlation between PC1s and low latitude EAWM wind indices than the others of mid-high latitudes is the modulation with other active climate features such as ENSO. It plays a role on the maritime continent during the winter monsoon (Juneng, 2005). Whereas, the correlation between the index derived from mid-latitude (EAWM-M) wind and PC1s is close to the correlations with indices derived from SLP. This is reasonable because the SLP gradient is related to SH forcing, which is the major active climate feature influencing SLP and wind along the East Asia coast (Wu, 2002).

Among correlations of PC1s with the indices, it was found that the correlation coefficient of PC1s to the UMI index is highest. Therefore, the UMI index is the best index to reveal the wintertime wind variability over the IDP. Nevertheless, PC1sec shows a little higher significant correlation to EAWM indices (six of eight values) than that of PC1pri (Table 3.2). To represent a connection of wintertime northeasterly wind over the IDP to EAWM, PC1sec is a little better than PC1pri, and have a better connection to EAWM over the low-latitude than the mid-high latitude. For the second mode, PC2s does not show significant correlations with EAWM indices, comparing to the first leading PC. This indicates that the prevailing easterly wind over the southern IDP given by the Mode2 does not significantly correlate with the EAWM.

Table 3.2: Correlation coefficients between PCs and EAWM indices and related information

Index	PC1pri	PC1sec	PC2pri	PC2sec	Parameter
EAWMI*	0.56[a]	0.60[a]	−0.46[a]	−0.21	*v* (10 m)
EAWM-M*	0.33	0.35	−0.11	0.01	*v* (1000 hPa)
EAWM-L*	0.54[a]	0.59[a]	−0.20	−0.23	*v* (1000 hPa)
VI*	0.58[a]	0.59[a]	−0.23	−0.37	*v* (1000 hPa)
UMI*	0.76[a]	0.72[a]	−0.09	−0.43[b]	*v* (1000 hPa)
MI1	0.46[b]	0.44[b]	−0.14	−0.34	SLP
MI2	0.30[b]	0.31[b]	−0.24	−0.33	SLP
U300	0.34	0.38[b]	−0.42[b]	−0.33	*u* (300 hPa)

a and b denote significant levels at 0.01 and 0.05, respectively.

u and v denote zonal and meridional winds, respectively.

* denotes the index values were multiplied by −1 to keep the meaning of meridional wind moving southward when it is positive.

A possible cause of higher correlation between PC1s and low latitude EAWM wind indices than the others of mid-high latitudes is the modulation with other active climate features such as ENSO. It plays a role on the maritime continent during the winter monsoon (Juneng, 2005). Whereas, the correlation between the index derived from mid-latitude (EAWM-M) winds and PC1s is close to the correlations with indices derived from SLP. This is reasonable because the SLP gradient is related to SH forcing, which is the major active climate feature influencing SLP and the winds along the East Asian coast (Wu, 2002). For the second mode, most of correlation coefficients do not show significant correlations with EAWM indices. This indicates that the Mode2 is not significantly related to the EAWM.

3.4 Summary

Over the IDP, this section revealed spatio-temporal wintertime wind variability and identified the principal modes of the wind at 850 hPa by using the EOF analysis for complex numbers. The spatial patterns given by regression of wind on the primary and secondary components of the leading PC show prominent northeasterly wind over the IDP that agrees with the characteristic of the EAWM and its influence on the tropical region.

Namely, these results are consistent with the circulation characteristic of EAWM exhibiting wind blowing along the coast of East Asia and the influence of the Borneo vortex. Thus, the first mode of wintertime wind variability over the IDP affected by the EAWM via the wind blowing passes through the SCS to the IDP, whereas the second one is the equatorial easterly mode, which does not agree with the characteristic of EAWM. Therefore, the first mode appears to have a significant role in regulating climate conditions over different areas of the IDP than the second EOF mode. For this reason, this section presented the examination on possible connection of wintertime low-level wind variability over the IDP to the EAWM on the basis of the correlations between PCs and EAWM indices.

The first mode shows good correlations with the EAWM indices characterized by low latitude wind than do others. The comparison of correlations between PC1s and EAWM indices indicates that the UMI index is a suitable EAWM index to reveal the variability of the winter monsoon over the IDP. Thus, the influence of EAWM on the IDP related to wind blowing along the East Asia coastline, passing the SCS, and penetrating to the IDP. Hence, the relation of PC1s to EAWM indices is not fully correlated. Thus, there is another possible forcing on this mode. Whereas the second mode presents non significant correlation with the EAWM indices, indicating that the variability corresponding to the second mode does not influenced by the EAWM. Further analysis emphasizes on the first EOF mode to give more understanding and explore relation of wintertime northeasterly wind over the IDP to another climate forcing.